Title

Seamless multimaterial 3D liquid-crystalline elastomer actuators for next-generation entirely soft robots

Journal

Science Advances, 6(9)

ISSN

2375-2548

Authors

Zhang, Yubai
Wang, Zhenhua
Yang, Yang
et al.

Publication Date

2020-02-28

DOI

10.1126/sciadv.aay8606

MATERIALS SCIENCE

Seamless multimaterial 3D liquid-crystalline elastomer actuators for next-generation entirely soft robots

Yubai Zhang[1]*, Zhenhua Wang[1]*, Yang Yang[1], Qiaomei Chen[1], Xiaojie Qian[1], Yahe Wu[1], Huan Liang[1], Yanshuang Xu[1], Yen Wei[1,2†], Yan Ji[1†]

Liquid-crystalline elastomers (LCEs) are excellent soft actuator materials for a wide range of applications, especially the blooming area of soft robotics. For entirely soft LCE robots to exhibit high dexterity and complicated performance, several components are typically required to be integrated together in one single robot body. Here, we show that seamless multicomponent/multimaterial three-dimensional (3D) LCE robots can be created via simultaneously welding and aligning LCE materials with different chemical compositions and physical properties without other additives such as tapes and glues (just like metal welding). Both welding and aligning of the LCE materials rely on thermal polymerization of preformed LCE films with reactive acrylate groups. This method provides an easy way to robustly fabricate arbitrary 3D desirable geometries with strongly stable reversible actuations and multifunctionalities, which greatly enlarges and benefits the future applications and manufacturing of LCE soft robots.

INTRODUCTION

Entirely soft robots, which are completely made of soft components, are of particular interests in the nascent area of soft robotics since they can provide safer human interaction, adapt to unpredictable environments, produce high specific power when actuated, and eliminate possible recurring failure compared to hybrid soft-rigid systems, presenting exceptional opportunities for various disciplines such as biomedicine, tissue engineering, and aeronautics (*1*–*9*). Stimuli-responsive materials are promising candidates for entirely soft robots because they have the potential to integrate sensors, actuators, and their control systems in the three-dimensional (3D) soft supportive bodies (*2*, *7*). Among all stimuli-responsive materials, liquid-crystalline elastomers (LCEs) are particularly attractive owing to their extraordinary reversible shape-changing properties when exposed to various stimuli (*10*–*15*).

For future fabrications and applications of LCE robots, one critical but unaddressed issue is to integrate several components, especially multiple materials with distinctive functions, and coordinate inside the entirely soft robot body so as to carry out sophisticated operations. For instance, in robotic systems with other types of soft actuators, some require both high stiffness and low stiffness to undertake different roles (*3*, *5*, *6*). Upon integration, the soft low-stiffness parts can perform large actuation strain to change the 3D shapes on demand to passively adapt to variable environments, while the relatively rigid parts can provide high precision and generate or sustain high force to actively produce external work and complete complicated tasks. Thus, it is substantially important to create multicomponent and multimaterial entirely soft LCE robots to improve their dexterity and flexibility and enlarge their functionalities and applications. Unfortunately, the existing 3D reversible LCE structures are almost all composed of single material due to the inherent restriction of the materials or the limitations of fabrication techniques. We emphasize that the "multicomponent" and "multimaterial" in our study refer to macroscopic heterogeneous multicomponent and multimaterial structures but not the composites that contain homogeneous (or microscopically heterogeneous) structures (e.g., LCE-carbon nanotube composites). Strictly speaking, we note that previously sporadic cases have used LCE bilayers to create heterogeneous structure (*16*–*22*). However, for all those bilayer structures, there is a fatal problem, which is that they can only combine two different materials to make the whole structure to perform simple bending-related actuations. It is intrinsically difficult for them to realize complex multimaterial structures in which different parts can perform different actuation behaviors and exhibit different functions. Besides, the actuation type of the bilayer structures is limited to bending-related movements, which restrict their motions and prevent them from fulfilling the urgent needs of designing complex LCE robots and enlarging their future applications.

Here, we show that multicomponent/multimaterial entirely LCE soft robots can be fabricated via simultaneously welding and aligning LCE materials with distinctive chemical components and physical properties. The successful welding and aligning both rely on permanent covalent bonds formed by thermal polymerization of reactive acrylate groups in preformed acrylate group–rich LCE films. The permanent covalent bonds formed by thermal polymerization of the acrylate groups not only ensure the robust welding between films but also assure the permanent macroscopic LC alignment, which guarantees the strong actuation stability of LCE actuators and their undisrupted actuation behavior after repeated use, thus lengthening their life span. The heterogeneity in the multimaterial LCE robots is realized by varying the chemical reactions and reagents used in the preformed acrylate group–rich films, as long as they can provide the mesogenic moieties and excess acrylate groups. These individual preformed acrylate group–rich films with different chemical compositions can be first mass produced and stored without the second-step thermal polymerization, since the first reaction that makes them is completely stopped. In the future, when needed, individual preformed acrylate group–rich films with different chemical components can be freely welded and aligned to form arbitrary desired multimaterial 3D robots, which can be beneficial for mass production in manufacturing. Not only can this technique enlarge the flexible designs (and functions)

[1]MOE Key Laboratory of Bioorganic Phosphorus Chemistry and Chemical Biology, Department of Chemistry, Tsinghua University, Beijing 100084, China. [2]Department of Chemistry, Center for Nanotechnology and Institute of Biomedical Technology, Chung-Yuan Christian University, Chung-Li 32023, Taiwan, China.
*These authors contributed equally to this work.
†Corresponding author. Email: jiyan@mail.tsinghua.edu.cn (Y.J.); weiyen@tsinghua.edu.cn (Y.We.)

of LCE soft robots and potentially enable mass production, which offers a new path for LCE robot manufacturing, but it can also improve material utilization and save resources by making use of leftover unaligned LCE small pieces, which will be important for the future applications of LCE soft robots.

RESULTS

The formation of multicomponent/multimaterial LCE structures is based on thermal polymerization of preformed LCE films containing reactive acrylate groups, forming permanent covalent bonds that can not only be used to fix macroscopic LC order, which is required for reversible LCE actuations, but also covalently join together two separate films. Photopolymerization of preformed LCE films with excess acrylate groups has been used in a few works to make monodomain LCEs (*23*–*28*). However, welding has not been realized in these works because ultraviolet (UV) light was used to initiate self-polymerization. UV light has limited the penetration ability, which results in the insufficient capability of welding. In addition, the energy produced by UV light is not enough for driving the polymer chains to move. In our study, to enable efficient welding, we use heat instead of UV light to initiate the polymerization. As illustrated and demonstrated in Fig. 1A, thermal polymerization of excess acrylate groups can be used alone to form permanent covalent bonds, which are capable of welding two preformed acrylate group–rich films together upon proper compression. Various initiators such as 2,2-azoisobutyronitrile (AIBN) can be used for thermal polymerization of acrylate groups. Meanwhile, as illustrated in Fig. 1B, thermal polymerization can also be used alone to fix macroscopic LC orientation to make reversible LCE actuators. The mechanism of thermal polymerization of acrylate groups is shown in Fig. 1C. Since the welding process and the monodomain-fabricating process are based on the same reaction, by conducting welding and aligning at the same time, multicomponent LCE structures can be obtained (Fig. 1D). We noticed that permanent covalent bonds have been used to achieve welding with "further amide-forming cross-linking reaction" (*29*), but the bonds in this paper are restricted to weld the same type of material, which is also proposed in this paper as "self-welding." On the contrary, the concept of joining LCE actuators with different chemical compositions and even completely different chemical networks to form heterogeneous structures to combine different physical properties in one entirety and achieving advanced multiple functions, was extremely difficult to be implemented in the past.

The heterogeneous chemical compositions in the multicomponent/multimaterial LCE structures are achieved by adjusting the chemical reactions involved in synthesizing the preformed acrylate group–rich films. They can be formed by any reactions as long as they can build the LC network and provide excess reactive acrylate groups. Here, we choose an unequimolar base-catalyzed thiol-acrylate reaction due to its rapidity and low sensitivity to oxygen inhibition. To fabricate multimaterial LCE soft robots, in this paper, we first prepare six different acrylate group–rich LCE films with different chemical components (namely, pre–LCE 1, pre-LCE 2, pre-LCE 3, pre-LCE 4, pre-LCE 5, and pre-LCE 6) based on thiol-acrylate chemistry, which has been widely used to construct LCEs in the past (*23*, *24*, *28*, *30*–*35*). Pre-LCE 1, whose starting materials are shown in Fig. 2A, is normally used as an example for most demonstrations unless otherwise noted. The successful synthesis of preformed acrylate group–rich films is proved by the infrared (IR) spectroscopy and swelling experiments. IR spectroscopy shows that the thiol group peak (2568 cm^{-1}) vanishes after cross-linking (fig. S1A), while the acrylate group peak (815 cm^{-1}) did not completely disappear (fig. S1B), indicating that the thiol-acrylate click reaction happens and stops when all thiol groups are consumed, leaving excess acrylate groups. Notably, the excess acrylate groups existed in preformed films because the molar of the acrylate groups exceeds the molar of total thiol groups by 15%. The swelling experiment is performed in solvent dichloromethane (DCM) at room temperature and gives a gel fraction of 91.1%, which proves the existence of a chemically cross-linked network (fig. S1, C and D).

The so-called polydomain LCEs (*10*), which are LCEs without macroscopic mesogen alignment, are achieved by simply heating the preformed acrylate group–rich films at 80°C for 24 hours, allowing the thermal polymerization of acrylate groups to take place. IR images of the samples before and after thermal polymerization (fig. S2A) show that the acrylate group peak at 815 cm^{-1} vanishes after heating, which means the excess acrylate groups are consumed, indicating the self-polymerization of acrylate groups happens while heating. The thermal analysis of polydomain LCE 1 is shown in the Supplementary Materials (fig. S2, B to D).

The so-called monodomain LCEs whose mesogens are macroscopically aligned (*10*) can be formed by stretching the samples and then fixing the LC orientation by thermal-initiated AIBN-induced self-polymerization of acrylate groups. Since the reaction used to form the preformed acrylate group–rich LCE films (thiol-acrylate reaction) and the reaction used for aligning (thermal polymerization of acrylate groups) happen at different temperatures and are independent of each other, this method decouples the "network-forming" process and "aligning" process, which offers better control of the whole process compared with using the traditional two-step cross-linking method. In addition, our preformed acrylate group–rich LCE films are dry and fully developed LCE materials whose strain at break (250%) is much larger than the strain needed to align the mesogens (130 to 140%), which makes it easier to stretch and align the sample without breaking them. Our method can effectively raise the successful rate of the monodomain fabrication and lower the difficulty of controlling the whole process. IR spectroscopy (Fig. 2B) shows that the acrylate group peak at 815 cm^{-1} vanishes after the monodomain formation, indicating that the thermal polymerization of acrylate groups happens during the mesogen-aligning process. The order in monodomain LCE 1 is confirmed by x-ray diffraction (XRD) experiments (Fig. 2C, left), which shows two bright spots indicating the sample is oriented, while the XRD pattern of the polydomain LCE 1 is a diffuse ring, indicating that the sample is unoriented (fig. S2E). The corresponding intensity versus azimuthal angel figure of monodomain LCE 1 is shown in fig. S3. Other proof of the formation of monodomain LCE 1 can be found in fig. S4. Monodomain LCE 1 can contract at the isotropic phase and elongates at the anisotropic phase reversibly (Fig. 2C, right), which shows the temperature-responsive actuation behavior. In addition to the simple contraction-elongation movements, different 3D reversible actuation modes can also be easily obtained by simply manipulating the film sample with the aid of molds or Teflon tubes, which greatly enlarges the motion modes that can be used to create the soft robots. Figure 2 (D and E) shows five different actuation modes changing shapes reversibly between the anisotropic state and the isotropic state.

The actuation stability is critical for soft robots composed of LCE actuators since strongly stable actuations extend the service life of LCE robots, which hugely contribute to their future applications.

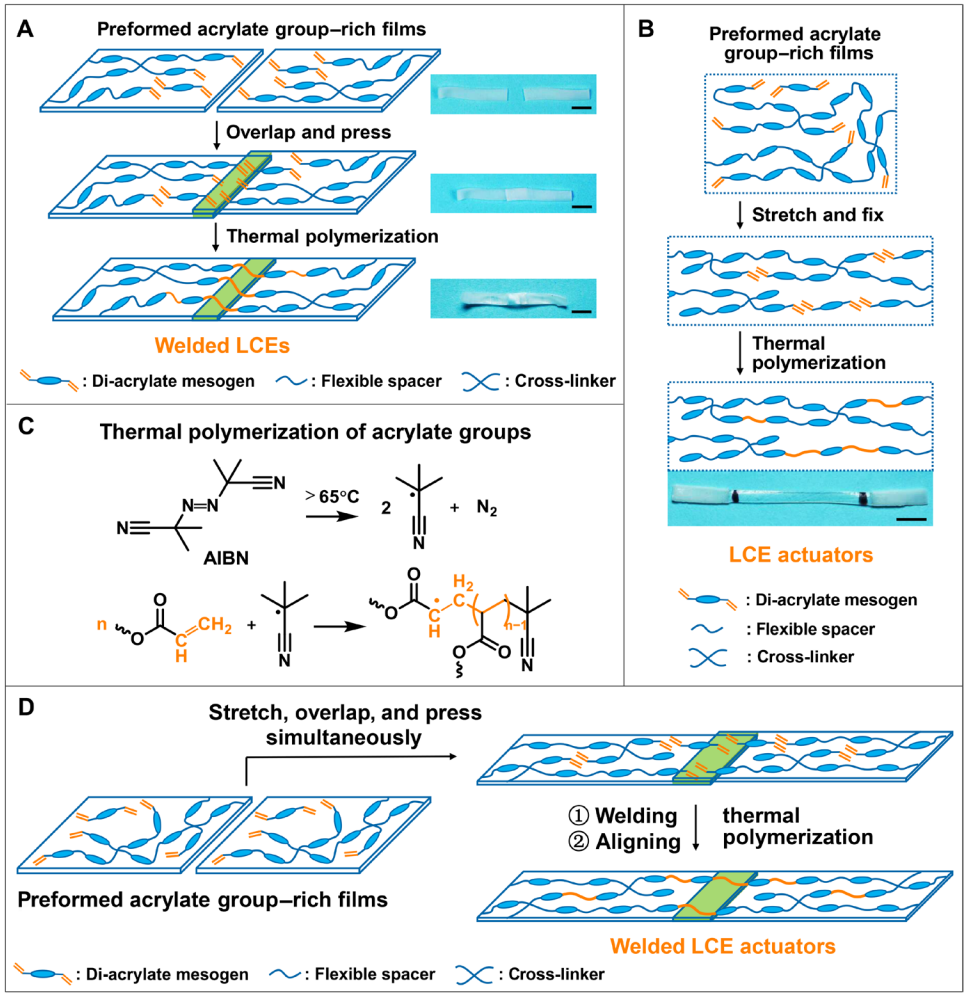

Fig. 1. Illustration of welding of preformed acrylate group–rich films and formation of monodomain LCE actuators and welded LCE actuators via thermal polymerization of preformed acrylate group–rich films. (**A**) Scheme of welding preformed acrylate group–rich films alone. (**B**) Scheme of formation of monodomain LCE actuators alone. (**C**) Mechanism of thermal polymerization of acrylate groups. (**D**) Scheme of the simultaneously "welding" and aligning processes to realize the formation of welded LCE actuators. Scale bars, 5 mm. (Photo credit: Yubai Zhang, Tsinghua University.)

Compared with LCEs aligned by exchangeable links, LCEs orientated with permanent covalent bonds have distinctive merit in terms of actuation stability. The actuations of LCEs aligned with exchangeable links suffer from the risk of instability when exposed to relatively high temperature because of fast breaking and reforming of bonds, or the LC order will gradually be diminished after repeated use as the exchangeable reactions can happen slowly at ambient conditions and cause the LC order to gradually be disrupted and eventually disappear. On the contrary, in our method, once the permanent bonds are formed, they are unlikely to break, thus robustly and permanently fixing the macroscopic LC orders, which results in strong actuation stability. In Fig. 2F, one can see that 64 and 61% actuation strains are achieved before and after 1000 cycles of temperature varying between 20°C (anisotropic phase) and 100°C (isotropic phase), respectively, indicating that the resulting LCE actuator had a strong stable actuation behavior.

As illustrated in Fig. 1A before, welding of the preformed acrylate group–rich films can be achieved by applying proper force on the overlapped region and heating them. Upon heating, the excess acrylate groups in the overlapped area undergo heat-induced thermal polymerization, and they form strong permanent covalent bonds to weld preformed samples. To prove that this reaction happens during the welding process, we used IR spectroscopy to compare IR images of the welded samples after welding (the overlapped area) with the preformed acrylate group–rich films before welding (fig. S5A). It can be seen that the acrylate double bond peak at 815 cm^{-1} disappears after welding, which means that at least most of the 15 mole percent (mol %) excess acrylate groups are consumed and react to form equivalent new permanent covalent bonds. To evaluate the welding effect of the newly formed permanent covalent bonds, we first conducted cross-sectional scanning electron microscopy (SEM) to directly observe the samples before and after welding (Fig. 3A). SEM images of the overlapped films before heating show an obvious seam between the two films, while SEM images of the films after thermal polymerization show a total fusion and no seam, which proves that the permanent covalent bonds achieve seamless welding. Tensile tests are conducted to evaluate the mechanical strength of the welded sample compared with the original materials. Stress-strain curves of the original polydomain sample and the welded sample are shown in fig. S5B. It can be seen that after welding, the stress-strain

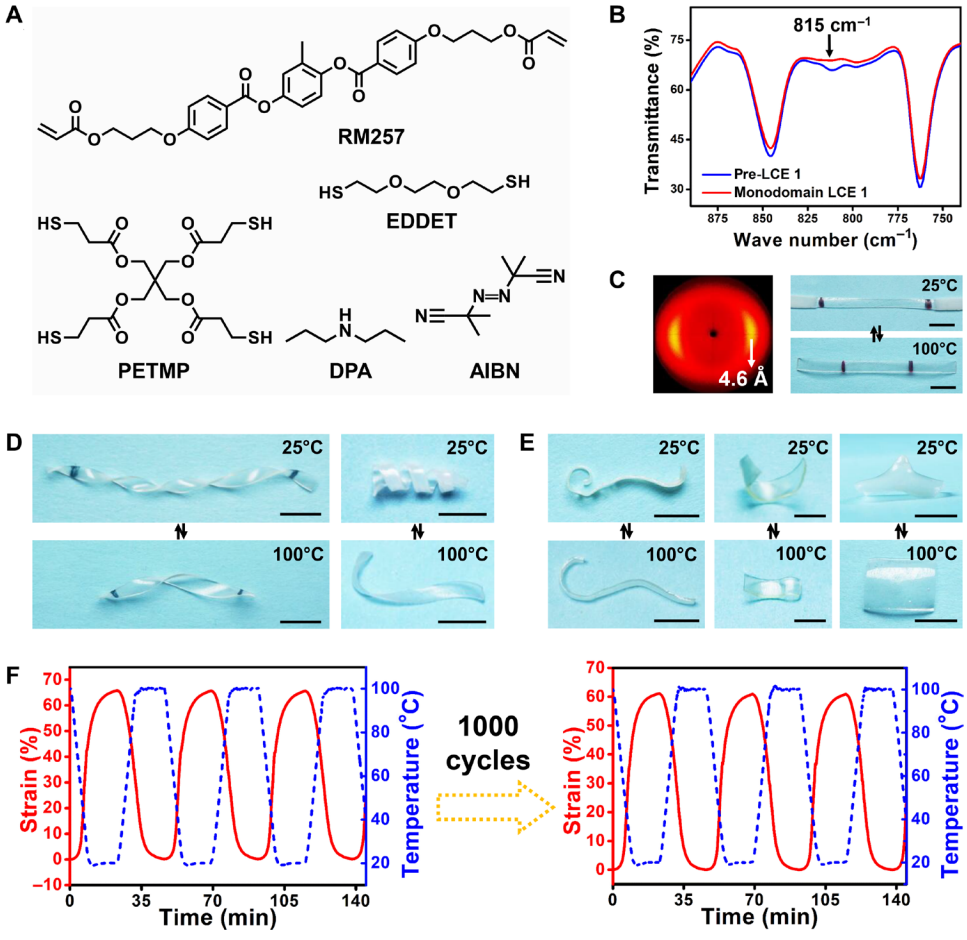

Fig. 2. Formation and characterization of monodomain LCE actuators and their different actuation modes. (**A**) Reagents used in pre-LCE 1. (**B**) IR spectroscopy of pre-LCE 1 and the monodomain LCE 1. (**C**) XRD patterns of monodomain LCE 1 (left); monodomain LCE elongated and contracted reversibly (right). (**D**) Winding and unwinding of the spiral ribbon (left) and spiral spring (right). (**E**) Curling and uncurling (left); bending and unbending (middle); pin-shaped and flat configurations (right). (**F**) The actuation strain of monodomain LCE 1 before and after 1000 cycles of actuations measured by dynamic mechanical analysis (DMA). Scale bars, 5 mm. (Photo credit: Yubai Zhang, Tsinghua University.)

curve is not exactly overlapped with the original polydomain sample. We found that the bonding area changed from opaque to transparent (the photos are shown in fig. S5C) when applying forces on the sample and heating, which means that alignment forms during the bonding under pressure. Since the stress-strain curves of the aligned LCEs are very different from the unaligned ones, it is understandable that the stress-strain curve after welding is not exactly the same with the original polydomain sample. Despite the above, when the welded sample is stretched to fracture, it breaks at the bulk material but not within the overlapped region, which indicates successful welding. Swelling experiments of the welded samples are also conducted to test the strength of the permanent covalent bonds (fig. S5D). The welded LCEs can survive swelling tests, followed by drying.

By welding preformed acrylate group–rich films and aligning LC order in them at the same time (since the two individual operations are based on the same principle and experience the same process), very complex and arbitrary 3D LCE actuators containing heterogeneous alignment in different areas, which can mimic complicated machine and animal movements, can be directly obtained. The multicomponent LCE actuators in which different parts can exhibit different actuation modes are shown in Fig. 3B. The resulting multicomponent actuators can exhibit heterogeneous actuation and shape shifting between the anisotropic phase and the isotropic phase reversibly. A windmill-shaped reversible LCE structure capable of moving its "wings" and transforming between a boomerang shape (anisotropic phase) and a windmill shape (isotropic phase) is fabricated by simultaneously welding and aligning the wings (Fig. 3C). A fan-simulating reversible LCE robot is fabricated by combining a helix reversible structure and three trapezoidal actuation-free films together. Beyond imitating the fan geometries, the typical rotating movements are also simulated as the temperature changes, since the helix reversible structure on the top winds and unwinds reversibly, producing twisting force to drive the "blades" rotating, converting heat into mechanical work (Fig. 3D and movies S1 and S2). An "eight-leg" octopus–mimicking LCE robot capable of rolling up and down its "legs" in response to heat, simulating the biological movements (Fig. 3E and movies S3 and S4), is fabricated. Welding is not only used in this "octopus" to construct the 3D backbone structure but also used to attach a "separate leg," which allows healing for an "injured seven-leg octopus." The illustrations of the detailed fabrication methods of each structure can be found in fig. S6.

Not only can LCE materials with the same chemical components be joined together, but soft elementary parts that are chemically

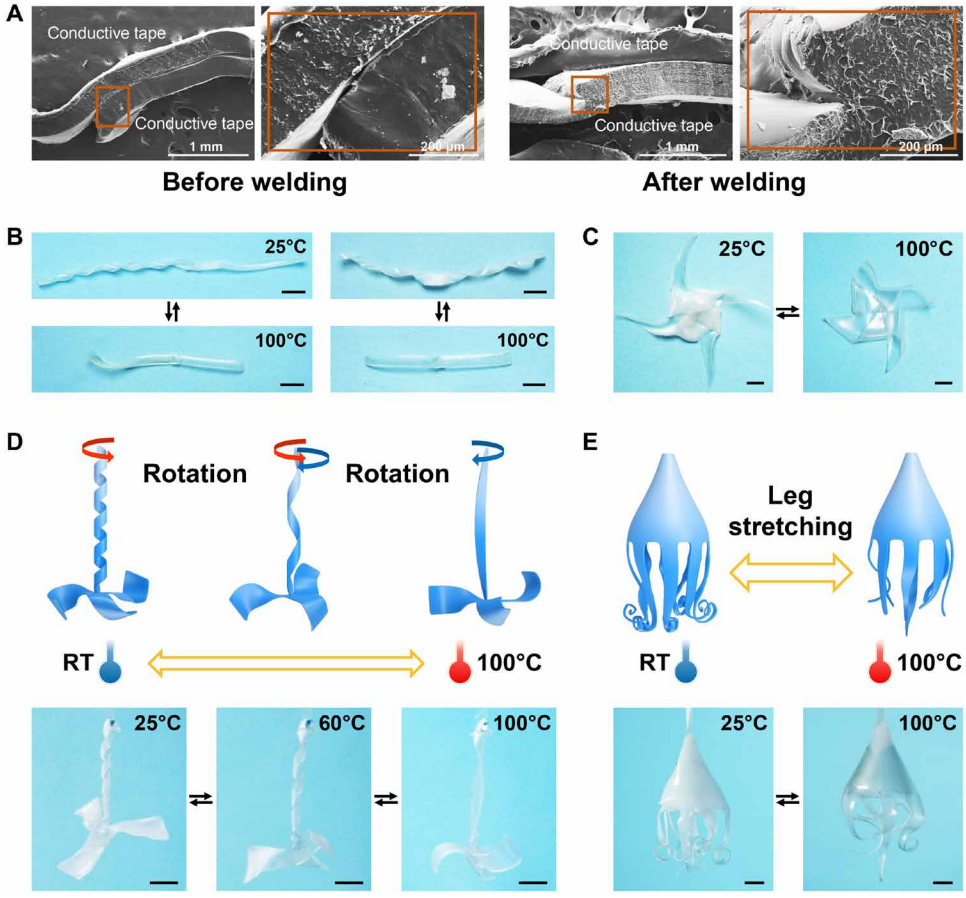

Fig. 3. Proof and illustration of formation of very complicated 3D machine- and animal-mimicking LCE actuators. (**A**) SEM images of pre-LCE 1 films before (the left two figures: scale bars, 1 mm and 200 μm) and after (the right two figures: scale bars, 1 mm and 200 μm) welding. (**B**) Welded reversible structures with the left part being a ribbon-like spiral reversible structure and the right part being a contraction-only reversible structure (left); two reverse ribbon-like spiral reversible structures (right). (**C**) Windmill-shaped reversible structure. (**D**) Schematic showing and photographs of a reversible fan-like structure rotating. (**E**) Schematic showing and photographs of a reversible eight-leg octopus-like structure stretching legs. RT, room temperature. (Photo credit: Yubai Zhang, Tsinghua University.)

different can also be connected via permanent covalent bonds and assembled. This method is not limited to combining two chemically different samples, but three or even more samples with different chemical components can be joined together. Combining LCE materials with different chemical components can install different physical properties in different areas in one entirety and bring previously unexplored advanced functions to the LCE soft robots. Multistage reversible shape-changing LCE actuators are obtained by welding LCEs with different anisotropic-isotropic temperatures (T_i) (Fig. 4A). To illustrate the multistage reversible shape-changing effect, pre-LCE 2 and pre-LCE 3 are synthesized by varying the difunctional spacer in pre-LCE 1. Figure 4A shows the welded LCE actuator composed of three-helix reversible structures with different T_i made from pre-LCE 1, pre-LCE 2, and pre-LCE 3 and illustrates the stage-by-stage reversible actuation when temperature rises step by step from room temperature to 145°C and back to room temperature. DMA experiments are conducted to observe the T_i of polydomain LCE 2 and polydomain LCE 3 (fig. S7). The composite structures we illustrated here can reversibly change their shapes between four structures, but this method is not limited to four. By combining more than three LCEs with different T_i, theoretically, reversible shape changing between unlimited numbers of structures can be expected. This multistage reversible shape-changing structure allows the soft robots to change step by step according to external environment and can be used in areas where reversible shape changes between multiple shapes are needed.

The strategy presented here also makes it possible to join together materials with different functions to create multifunctional LCE actuators with permanent covalent bonds, which is difficult to realize in the past. LCE actuators that can partially respond to both IR light and heat and partially respond to heat only reversibly can be fabricated by welding (aligning at the same time) together one LCE doped with polydopamine nanoparticles (pre-LCE 4) and one without (pre-LCE 1) (Fig. 4B). When IR light is switched between on and off, only the area with polydopamine can unwind and wind reversibly because of the photothermal effect of polydopamine nanoparticles (Fig. 4B, a and b, and movie S5). When IR light is off and temperature varies between 25° and 100°C, the whole structure responds to heat reversibly (Fig. 4B, c and d). The supplementary characterizations of the photothermal effect of the whole structure can be found in fig. S8. This area-selective multiresponsiveness comes in handy when the soft robots are needed to be exposed to a homogeneous environment where selective stimuli are not available and only a certain region of the soft robots is required to actuate.

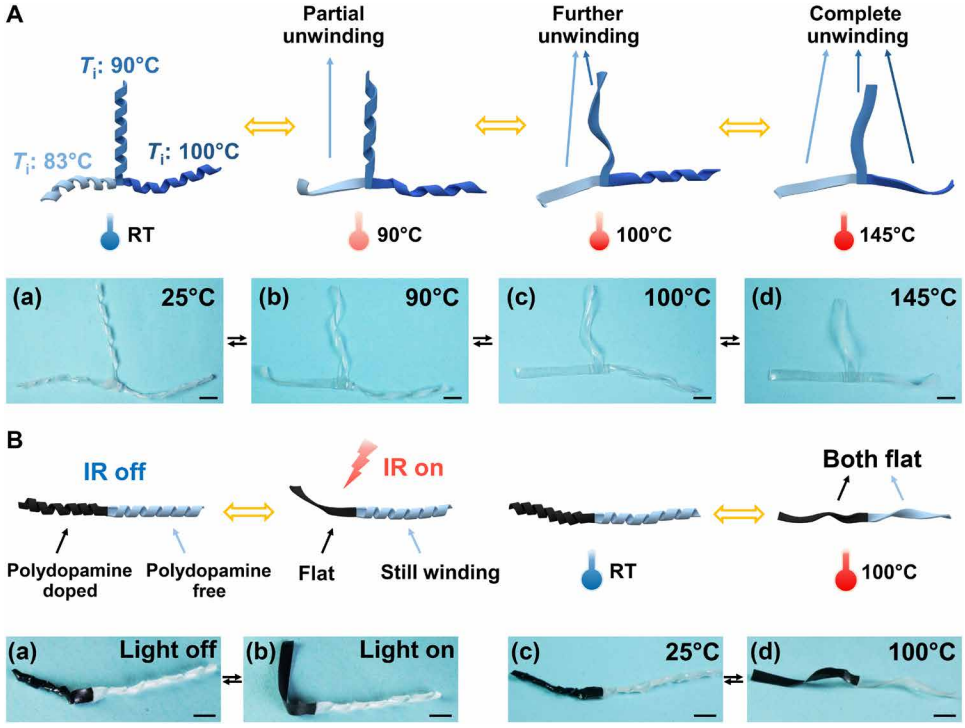

Fig. 4. Multifunctional multimaterial LCE actuators in which different parts contain different chemical components. (**A**) Schematic showing and photographs of a multistage reversible structure. (**B**) Schematic showing and photographs of an area-selective reversible multiresponsive structure. Scale bars, 5 mm. (Photo credit: Yubai Zhang, Tsinghua University.)

LCE materials with completely different chemical components and network structures can also be joined together via our method. Pre-LCE 5 is a (mercaptopropyl)methylsiloxane homopolymer (PMMS)–based side-chain LCE, and the reagents and network structure of pre-LCE 5 are shown in Fig. 5A. Additional proof of successful welding of two markedly different material systems (pre-LCE 1 and pre-LCE 5) are given in fig. S9. SEM images of the overlapped films show that the obvious seam between two materials before welding (fig. S9A) disappears after the thermal polymerization happens (fig. S9B), resulting in a totally fused seamless integrate. IR images of the overlapped region show that the acrylate double bond peak at 815 cm^{-1} disappears after welding, which means that the excess acrylate groups are consumed and react to form new permanent covalent bonds (fig. S9C). The welded LCEs can survive swelling tests, followed by drying (fig. S9D). Figure S9E shows that when the welded sample is stretched to fracture, it breaks at the bulk material but not within the overlapped region, which indicates successful welding. Figure S9F shows the stress-strain curves of the original polydomain LCE 1, original polydomain LCE 5, and the welded sample. Since the welded sample is composed of three different materials (including the polydomain LCE 1 part, the polydomain LCE 5 part, and the overlapped part), it is reasonable that the stress-strain curve of the welded sample is different from the typical polydomain stress-strain curve. Because of the same reason, it is also understandable that the curve of the welded sample is different from the curve of either the original polydomain LCE 1 or the original polydomain LCE 5. Multimaterial 3D actuators can be achieved by welding and aligning preformed acrylate group–rich films with completely different chemical networks. A composite reversible structure made from pre-LCE 1 and pre-LCE 5 capable of responding to heat is shown in Fig. 5B. Apart from pre-LCE 5, we also synthesize a pre-LCE 6, which is a different PMMS-based side-chain LCE, to further illustrate the welding of markedly different LCE materials. The chemical composition of pre-LCE 6 and the obtained heat-responsive multimaterial helix actuators made from pre-LCE 1 and pre-LCE 6 are shown in fig. S10 (A and B, respectively). Since different categories of LCEs (e.g., side-chain LCEs and main chain LCEs; nematic LCEs and cholesteric LCEs) are in possession of distinctive properties, being able to take elementary LCE building blocks with different prepossessed inherent functions and simply seamlessly assemble them whenever and wherever they are wanted in one structure intrinsically and efficiently endows the resulting LCE robots multiple functions that are desired, which is substantial for future LCE robot design and can extend the applications of LCE robots into previously impossible territories.

DISCUSSION

We have presented a practical and simple strategy to form seamless multimaterial LCE soft robots in which different parts of the robot are in possession of different chemical compositions and physical properties. Since the strategy is based on permanent covalent bonds formed via thermal polymerization of preformed acrylate group–rich films, it lacks the ability to repeatedly reprogram the structures. On the flip side, the permanent bonds that were used to realize welding and fabricating monodomain LCE actuators endow very strong actuation stability, which highly extends the durability of the LCE robots, improving qualities of the future corresponding products and potentially saving costs. By introducing various chemistries and multiple actuation modes, LCE materials with different physical properties, chemical compositions, and even completely different

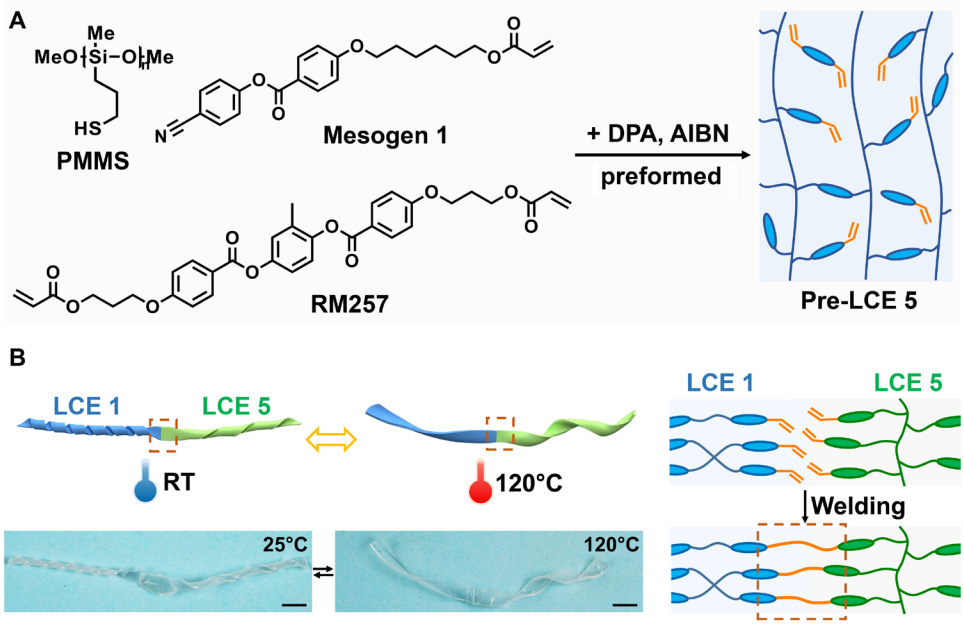

Fig. 5. The chemical network of pre-LCE 5 and the multimaterial actuator made from pre-LCE 1 and pre-LCE 5. (**A**) Reagents (left) and the network structure (right) of pre-LCE 5. (**B**) Schematic showing and photographs of the heat-responsive multimaterial actuator made from pre-LCE 1 and pre-LCE 5 (left); illustration of welding from pre-LCE 1 and pre-LCE 5 (right). Scale bars, 5 mm. (Photo credit: Yubai Zhang, Tsinghua University.)

chemical networks are fabricated and welded together (while aligning) to obtain complicated machine- and animal-imitating 3D reversible LCE structures and other multifunctionalities (e.g., multistage reversible shape-changing effect, area-specific multiresponsiveness), which greatly benefits the flexible design and dexterity of LCE robots. In addition, this strategy can also be used as a potential mass production method in future manufacturing. After the preformed acrylate group–rich films form, there is no rush to continue the second reaction to align or weld them. They can be first mass produced in many different kinds (with different chemical reactions) and then stored in proper condition without further processing. In the future, they can be taken out as needed (either to be a static support without actuation or to be further aligned to perform actuation) and freely combined (welded and aligned) to form desired 3D multimaterial LCE structures. This method allows for storing different LCE elementary parts in the form of films instead of already-formed complicated shapes, which effectively lessens the difficulty of storage and saves storage space, which can be beneficial for future manufacturing. This technique can be further generalized to multiple systems and offer the potential for other distinctive reactions (beyond thiol-acrylate chemistry) to create additional exceptional functions in the actuators (not limited to LCEs). In this way, it promises to contribute importantly to the development of future multifunctional smart soft robots and other device applications.

MATERIALS AND METHODS

Materials

RM257 (98%, Shijiazhuang Sdynano Fine Chemicals), 3,6-dioxa-1,8-octanedithiol (EDDET) (97%, TCI), 1,3-dimercaptopropane (98%, Energy Chemical), 1,2-ethanedithiol (99%, TCI), pentaerythritol tetra(3-mercaptopropionate) (PETMP) (95%, Energy Chemical), and dipropylamine (DPA; Amethyst Chemicals) reagents were used as received without further purification. AIBN (98%, Maya Reagent) was used after recrystallization. Polydopamine nanoparticles were synthesized according to previous work (*20*). PMMS (Gelest Inc.), 4-(6-acryloyloxyhexyloxy)-benzoesure (4-cyanophenylester) (named mesogen 1; 97%, Jinan Tai Er Pu Chemical Company in China), tetrahydrofuran (THF) (Bei Jing Tong Guang Fine Chemicals Company) were also used as received.

Synthesis of preformed acrylate group–rich films (pre-LCE 1, pre-LCE 2, pre-LCE 3, pre-LCE 4, pre-LCE 5, and pre-LCE 6)

Pre-LCE 1 films were formed using a base-catalyzed thiol-acrylate Michael addition reaction. RM257 (0.05 g, 0.92 mmol) was chosen as a diacrylate mesogen, while both EDDET (0.09 g, 0.48 mmol, difunctional flexible spacer) and PETMP (0.08 g, 0.16 mmol, tetrafunctional cross-linker) were selected to provide thiol groups (40 mol % of the thiol groups belonged to PETMP). DPA (10 μl) was selected as the catalyst. The molar of the acrylate groups exceeded the molar of the total thiol groups by 15%, and the molar ratio of EDDET to PETMP was 3:1. RM257 was first dissolved in THF at room temperature under vortex with a mass ratio of RM257 to THF being 1:8.87. After RM257 was totally dissolved, EDDET, PETMP, and AIBN were added to the solution and mixed well. Last, DPA [1 weight % (wt %) of all reactants] was added into the solution and mixed before the resulting solution was quickly poured into the molds (4 cm × 4 cm × 0.5 cm). Noticeably, AIBN was preloaded in pre-LCE 1 as the initiator to later induce the free radical thermal polymerization between excess acrylate groups. The molds were composed of Teflon, and the shape was not limited and could be designed as required. The solution was then allowed to cure overnight, followed by vacuum drying to remove the remaining solvent. The resulting pre-LCE 1 was stored at 0°C to prevent the decomposition of AIBN.

Pre-LCE 2 films were formed by changing EDDET in pre-LCE 1 to 1,3-dimercaptopropane. The amounts of reagents used in pre-LCE 2 were RM257 (0.57 g, 0.97 mmol), 1,3-dimercaptopropane (0.06 g,

0.51 mmol), PETMP (0.09 g, 0.17 mmol), DPA (10 μl), and AIBN (3.6 mg). The rest of the procedures were the same as those in pre-LCE 1.

Pre-LCE 3 films were formed by changing EDDET in pre-LCE 1 to 1,2-ethanedithiol. The amounts of reagents used in pre-LCE 3 were RM257 (0.58 g, 0.99 mmol), 1,2-ethanedithiol (0.05 g, 0.51 mmol), PETMP (0.09 g, 0.17 mmol), DPA (10 μl), and AIBN (3.6 mg). The rest of the procedures were the same as those in pre-LCE 1.

Pre-LCE 4 films were obtained by doping pre-LCE 1 with polydopamine nanoparticles (14.3 mg, 2 wt % of all reactants). The rest of the procedures were the same as those in pre-LCE 1, and the polydopamine nanoparticles were added along with EDDET, PETMP, and AIBN.

Pre-LCE 5 films were side-chain LCEs and were prepared by completely different materials and methods. PMMS was chosen as a main chain polymer with reactive pendent thiol groups. Mesogen 1 and RM257 were selected to provide acrylate groups (74 mol % of the acrylate groups belonged to RM257). DPA was selected as the catalyst. The molar of the acrylate groups exceeded the molar of the total thiol groups by 30%, and the molar ratio of mesogen 1 to RM257 was 1:1.45. PMMS and mesogen 1 were first dissolved in THF at room temperature under vortex. Then, DPA (1 wt % of all reactants) was added into the solution and mixed. After that, the mixed solution was treated with nitrogen for 40 min before it was sealed and put in the 85°C oil bath, followed by a 36-hour reaction with stirring. After the first-stage reaction, RM257 and AIBN were added into the solution and mixed. Then, DPA was added again and the solution was mixed before it was quickly poured into the molds. AIBN was preloaded in pre-LCE 5 as the initiator to later induce the free radical thermal polymerization between excess acrylate groups. The solution was then allowed to cure overnight, followed by vacuum drying to remove the remaining solvent. The resulting pre-LCE 5 was stored at 0°C to prevent the decomposition of AIBN.

Pre-LCE 6 films were side-chain LCEs and were prepared by completely different materials and methods. PMMS and EDDET were chosen as the main chain polymer and the flexible spacer with reactive pendent thiol groups, respectively (33 mol % of the thiol groups belonged to PMMS). Mesogen 1 and RM257 were selected to provide acrylate groups (90 mol % of the acrylate groups belonged to RM257). DPA was selected as the catalyst. The molar of acrylate groups exceeded the molar of total thiol groups by 30%, and the molar ratio of mesogen 1 to RM257 was 1:4.5. PMMS and mesogen 1 were first dissolved in THF at room temperature under vortex. Then, DPA (1 wt % of all reactants) was added into the solution and mixed. After that, the mixed solution was treated with nitrogen for 40 min before it was sealed and put in the 85°C oil bath, followed by a 36-hour reaction with stirring. After the first-stage reaction, RM257, EDDET, and AIBN were added into the solution and mixed. Then, DPA was added again, and the solution was mixed before it was quickly poured into the molds. AIBN was preloaded in pre-LCE 6 as the initiator to later induce the free radical thermal polymerization between excess acrylate groups. The solution was then allowed to cure overnight, followed by vacuum drying to remove the remaining solvent. The resulting pre-LCE 6 was stored at 0°C to prevent the decomposition of AIBN.

Synthesis of monodomain LCE 1 with different actuation modes (strip actuators, ribbon-shaped actuators, spring-shaped actuators, curling actuators, bending actuators, and pin-shaped actuators)

Mesogens are orientated by stretching the preformed acrylate group–rich films uniaxially to 130% strain, then fixing the stretched length, and heating it at 80°C for 24 hours in vacuum. A strip pre-LCE 1 was stretched to a length of 130% of the original length and fixed on a Teflon sheet with Teflon tapes. The sample was then placed at 80°C for 24 hours with vacuum to form monodomain LCE 1. The resulting strip LCE actuator exhibited reversible shape changing in response to temperature.

A ribbon-shaped LCE actuator was formed by twisting a strip pre-LCE 1 sample while stretching it to a length of 150% of the original length and fixed on a Teflon sheet with Teflon tapes. The rest of the procedures were the same as those in fabricating strip LCE actuators.

A spring-shaped LCE actuator was formed by winding a strip pre-LCE 1 sample on a Teflon tube with 2-mm diameter (the following circle of spiral was placed next to the previous circle) while stretching it to a length of 150% of the original length and fixed with Teflon tapes. The rest of the procedures were the same as those in fabricating strip LCE actuators.

A curling LCE actuator was formed by in situ winding a strip pre-LCE 1 sample on a Teflon tube with 2-mm diameter (the following circle of spiral was placed covered the previous circle) while stretching it to a length of 150% of the original length and fixed with Teflon tapes. The rest of the procedures were the same as those in fabricating strip LCE actuators.

A bending LCE actuator was formed by winding a strip pre-LCE 1 sample on a Teflon tube with 5-mm diameter (the length of the strip sample was shorter than the girth of the Teflon tube) while stretching it to a length of 150% of the original length and fixed with Teflon tapes. The rest of the procedures were the same as those in fabricating strip LCE actuators.

A pin-shaped LCE actuator was fabricated by placing a square pre-LCE 1 sample on a die punch mold. The rest of the procedures were the same as those in fabricating strip LCE actuators.

Synthesis of welded LCEs

Two strip samples were placed overlapped and sandwiched by two glass sheets covered with Teflon tapes. The resulting sample was then fixed by binder clips to provide suitable and constant pressure and placed at 80°C for 24 hours in vacuum to allow the AIBN to generate free radicals and induce the self-polymerization of acrylate groups and form permanent covalent bonds, thus resulting in samples being welded. The forced applied on the samples can be adjusted by the kind and number of the binder clips.

Synthesis of 3D LCE actuators with different actuation modes

A multicomponent actuator with multiple actuation modes including ribbon-like spiral and only contraction was fabricated by placing overlapped two strip pre-LCE 1 samples and sandwiching them by two glass sheets covered with Teflon tapes. Meanwhile, one strip was twisted and stretched to a length of 130% of the original length, while the other strip was simply stretched to a length of 130% of the original length and fixed on a Teflon sheet with Teflon tapes. The sample was then placed at 80°C for 24 hours in vacuum to allow the AIBN to generate free radicals and induce the self-polymerization of acrylate groups, thus fixing the mesogen order and realizing welding at the same time. A combined actuator with two reverse ribbon-like spiral was fabricated using the same method as above except that, in this case, two strips were twisted inversely, instead of one was twisted and the other was stretched.

Synthesis of 3D LCE actuators with machine- and animal-imitating structures

A 3D windmill-shaped LCE structure was fabricated with the following method. A square pre-LCE 1 sample was cut from four corners along the diagonal to a point where the cut length equaled quarter-length of the diagonal. Four corners were folded to the center, which later were fixed at the center by being sandwiched between two glass sheets covered with Teflon tapes along with pressured binder clips. Meanwhile, the other four corners were stretched to a length of 130% of the original length and fixed on a Teflon sheet with Teflon tapes. The resulting sample was then placed at 80°C for 24 hours in vacuum. The "four wings" of the resulting reversible windmill-shaped structure exhibited two-way contraction-elongation shape memory behavior.

A 3D fan-imitating LCE actuator capable of fan-mimicking movements was fabricated with the following method. The vertex of one strip and three trapezoid pre-LCE 1 samples were placed overlapped and sandwiched by two glass sheets covered with Teflon tapes to give a fan-like 3D shape. Meanwhile, the strip sample was twisted while being stretched to a length of 150% of the original length and fixed on a Teflon sheet with Teflon tapes to form a helix actuator. The sample was then placed at 80°C for 24 hours in vacuum. The resulting reversible fan-mimicking structure could simulate ceiling fan to rotate in response to temperature.

An octopus-mimicking LCE structure capable of octopus-imitating movements was fabricated with the following method. A circle with seven triangles attached and a separated triangle were cut from a square pre-LCE 1 sample and were placed overlapped and sandwiched by two glass sheets covered with Teflon tapes. Meanwhile, the circle was cut from the periphery to the center and made into a cone (the edges were placed overlapped and sandwiched by two glass sheets covered with Teflon tapes) to make the octopus head. In the meantime, the eight triangles were rolled on individual thin Teflon tubes (the following circle of the spiral was placed and covered the previous circle) and fixed with Teflon tapes to fabricate the movable legs. The sample was then placed at 80°C for 24 hours. The resulting reversible 3D octopus-simulating structure was able to move its legs in response to temperature.

Synthesis of composite reversible structures with multistage shape-changing effect made from pre-LCE 1, pre-LCE 2 and pre-LCE 3

Three strip samples were cut from pre-LCE 1, pre-LCE 2, and pre-LCE 3 and were placed with their one end overlapped and sandwiched by two glass sheets covered with Teflon tapes. Meanwhile, the three strips were twisted, respectively, and all were stretched to a length of 150% of the original length and fixed on a Teflon sheet with Teflon tapes. The sample was then placed at 80°C for 24 hours in vacuum. Since the resulting helix LCE 1, LCE 2, and LCE 3 reversible structures had different T_i, the resulting composite structure had multistage reversible shape-changing effect and can exhibit stage-by-stage reversible shape changing in response to step-by-step temperature changes.

Synthesis and characterization of composite reversible structures with area-specific multiresponsiveness made from pre-LCE 1 and pre-LCE 4

Two strip samples were cut from pre-LCE 1 and pre-LCE 4 and were placed with their one end overlapped and sandwiched by two glass sheets covered with Teflon tapes. Meanwhile, the two strips were twisted, respectively, and all were stretched to a length of 150% of the original length and fixed on a Teflon sheet with Teflon tapes. The sample was then placed at 80°C for 24 hours in vacuum. Since the resulting helix LCE 4 part in the composite actuator was doped with polydopamine nanoparticles while the helix LCE 1 part was not, only the LCE 4 part in the resulting composite structure can shape change between the helix configuration and flat configuration responding to both light and heat, while the LCE 1–containing part can only respond to heat. Thus, the area-specific multiresponsiveness was achieved. Movie S5 shows the composite reversible structure responding to IR light.

Synthesis of composite reversible structures made from pre-LCE 1 and pre-LCE 5

Two strip samples were cut from pre-LCE 1 and pre-LCE 5 and were placed with their one end overlapped and sandwiched by two glass sheets covered with Teflon tapes. Meanwhile, the two strips were twisted reversibly, and all were stretched to a length of 150% of the original length and fixed on a Teflon sheet with Teflon tapes. The sample was then placed at 80°C for 24 hours in vacuum. The resulting reversible actuator with a heterogeneous chemical network can change shape in response to temperature.

Synthesis of composite reversible structures made from pre-LCE 1 and pre-LCE 6

Two strip samples were cut from pre-LCE 1 and pre-LCE 6 and were placed with their one end overlapped and sandwiched by two glass sheets covered with Teflon tapes. Meanwhile, the two strips were twisted reversibly, and all were stretched to a length of 150% of the original length and fixed on a Teflon sheet with Teflon tapes. The sample was then placed at 80°C for 24 hours in vacuum. The resulting reversible actuator with a heterogeneous chemical network can change shape in response to temperature.

IR spectroscopy

All IR data were collected on a PerkinElmer Spectrum 100 FT-IR Spectrometer. IR spectroscopy was used to observe the thiol groups (2568 cm^{-1}) and acrylate groups (815 cm^{-1}) before and after the preformed acrylate group–rich network formed to prove the formation of the initial network and the existence of the excess acrylate groups in the network, as well as to observe the disappearance of the acrylate groups (815 cm^{-1}) after the formation of polydomain LCEs, monodomain LCEs, and welded pre-LCE 1 and pre-LCE 5 (measured from pre-LCE 1 side) to prove the occurrence of thermal polymerization of acrylate groups.

Differential scanning calorimetry experiments of polydomain LCE 1

Differential scanning calorimetry (DSC) was performed on TA instruments Q2000 with a scanning rate of 20°C min^{-1} from −20° to 160°C after a pretreatment cycle that is varying the temperature from −20° to 160°C at a rate of 30°C min^{-1}. DSC was used to observe the T_g and T_i of polydomain LCE 1.

Thermogravimetric analysis of polydomain LCE 1

Thermogravimetric analysis (TGA) results were obtained on a TA-Q50 under air atmosphere. TGA was used to determine the degradation temperature of the polydomain LCEs.

Dynamic mechanical analysis

Dynamic mechanical analysis (DMA) results were acquired on a TA Instruments Q800 machine. DMA was used to evaluate the actuation stability of monodomain LCE 1 in the film-tension geometry under a constant load of 10 kPa (film dimensions were 9.33 mm × 2.12 mm × 0.19 mm), with the change of temperature from 20°C (anisotropic phase) to 100°C (isotropic phase) at a rate of 10°C min^{-1} periodically. Since measuring the actuation cycle directly on DMA for 1000 times was time-consuming and damaging to the machine, we first measured the first four cycles by DMA and put the sample in DSC, allowing the sample to be heated to 100°C (isothermal for 1 min) and cooled to 20°C (isothermal for 1 min) at a rate of 30°C min^{-1} for 1000 times and then measured again on DMA for four cycles. The 64 and 61% actuation strain were achieved before and after 1000 cycles of temperature changes, indicating that the resulting LCE actuator had stable actuation behavior.

DMA was also used to obtain the stress-strain curves of the original polydomain sample and the welded samples (including welding of same materials and different materials). They were conducted using controlled force mode with a force rate of 0.2 N min^{-1}.

DMA was also used to obtain the modulus-temperature and tan δ–temperature curves of polydomain LCE 1, polydomain LCE 2 and polydomain LCE 3 to determine their T_g and T_i, respectively. The curves were measured at 1-Hz frequency and 3°C min^{-1} heating rate from −40° to 200°C in tension mode. T_g was determined at the maximum of the tan δ-temperature curve, while T_i was determined at the minimum of the storage modulus curve (*24*).

XRD experiments

2D XRD images were obtained on a Bruker D8 Discover diffractometer. XRD experiments were conducted to confirm the mesogen order in polydomain and monodomain LCEs. The order parameter was calculated based on the Hermans-Stein orientation distribution function shown below

$$S = \frac{3 < \cos^2\phi > -1}{2} \quad (1)$$

$$< \cos^2\phi > = \frac{\int_0^{\frac{\pi}{2}} I(\phi)\sin\phi\cos^2\phi d\phi}{\int_0^{\frac{\pi}{2}} I(\phi)\sin\phi d\phi} \quad (2)$$

where S is the order parameter, ϕ is the azimuthal angle, and I is the intensity. The value of the order parameter was estimated to be 0.45 according to Eqs. 1 and 2.

Scanning electron microscopy

SEM images were obtained on an SU-8010 model. SEM was used to observe the seam before and after welding (including welding of LCEs with the same chemical networks and different networks).

Polarizing optical microscope images of monodomain LCE 1

Polarizing optical microscopy (POM) images were acquired on a Nikon ECLIPSE LV100POL microscope equipped with a Nikon Digital Sight DS-U3 camera, purchased from Beijing Ruich Allway Instrument Technology Co. Ltd. POM was used to observe the optical properties of monodomain LCE 1.

Photothermal effect of composite reversible structures with arearea-specific multiresponsiveness containing LCE 1 and LCE 4

Temperature–power density curve of pre-LCE 4 was obtained by plotting the temperature against power density. IR light was emitted from a laser purchased at Hi-Tech Optoelectronics Co. Ltd. The light power was measured on an optical power meter. The temperature was measured with an FLIR-E64501 model. Power density was obtained by dividing light power by the light spot area.

Optical and thermal images of the composite reversible structure made from pre-LCE 1 and pre-LCE 4 were obtained on an IR camera. IR light with an intensity of 0.08 W cm^{-2} was used to irradiate the polydopamine-doped and polydopamine-free parts separately to see the change of temperature in the individual parts.

Swelling experiments

Swelling experiments of pre-LCE 1: The dimensions of the original preformed acrylate group–rich sample before swelling were 27.48 mm × 26.28 mm × 0.37 mm. After swelling in solvent DCM for 48 hours, the dimensions changed into 44.24 mm × 44.04 mm × 0.54 mm. The weight before swelling was 328.1 mg. The weight after swelling and vacuum drying was 298.8 mg.

Swelling experiments of welded LCEs (including welding of same materials and different materials): The swelling experiments for the welded LCEs were performed in solvent DCM for 12 hours (in a culture dish with tinfoil on the top to seal the dish and prevent the evaporation of the solvent). We then carefully dried the solvent very slowly by making the tinfoil on the dish a little loose leaving a minor gap.

SUPPLEMENTARY MATERIALS

Supplementary material for this article is available at http://advances.sciencemag.org/cgi/content/full/6/9/eaay8606/DC1

Fig. S1. Proof of the formation of pre-LCE 1.
Fig. S2. Additional characterizations of polydomain LCE 1.
Fig. S3. The intensity versus azimuthal angle figure of monodomain LCE 1.
Fig. S4. POM images of monodomain LCE 1 at room temperature being rotated at the interval of 45°.
Fig. S5. Additional proof of welding.
Fig. S6. Fabrication method of 3D machine- and animal-mimicking LCE robots.
Fig. S7. The modulus-temperature and tan δ–temperature curves of polydomain LCE 2 and polydomain LCE 3.
Fig. S8. Photothermal effect of combined structure contained pre-LCE 1 and pre-LCE 4.
Fig. S9. Proof of successful welding of pre-LCE 1 and pre-LCE 5.
Fig. S10. Welding of pre-LCE 1 and pre-LCE 6.
Movie S1. The temperature-responsive (from 30° to 100°C) rotation of the 3D fan-shaped reversible LCE structure.
Movie S2. The inverse temperature-responsive (from 100° to 30°C) rotation of the 3D fan-shaped reversible LCE structure.
Movie S3. The 3D octopus-imitating reversible robot uncurling legs upon temperature change from 30° to 100°C.
Movie S4. The 3D octopus-imitating reversible robot curling legs upon temperature change from 100° to 30°C.
Movie S5. The composite reversible structure made of LCE 1 (without polydopamine) and LCE 4 (with polydopamine) responding to IR light.

REFERENCES AND NOTES

1. M. Wehner, R. L. Truby, D. J. Fitzgerald, B. Mosadegh, G. M. Whitesides, J. A. Lewis, R. J. Wood, An integrated design and fabrication strategy for entirely soft, autonomous robots. *Nature* **536**, 451–455 (2016).
2. D. Rus, M. T. Tolley, Design, fabrication and control of soft robots. *Nature* **521**, 467–475 (2015).
3. N. W. Bartlett, M. T. Tolley, J. T. B. Overvelde, J. C. Weaver, B. Mosadegh, K. Bertoldi, G. M. Whitesides, R. J. Wood, A 3D-printed, functionally graded soft robot powered by combustion. *Science* **349**, 161–165 (2015).

4. M. Cianchetti, C. Laschi, A. Menciassi, P. Dario, Biomedical applications of soft robotics. *Nat. Rev. Mater.* **3**, 143–153 (2018).
5. G. M. Whitesides, Soft robotics. *Angew. Chem. Int. Ed.* **57**, 4258–4273 (2018).
6. F. Schmitt, O. Piccin, L. Barbé, B. Bayle, Soft robots manufacturing: A review. *Front. Robot. AI* **5**, 84 (2018).
7. L. Hines, K. Petersen, G. Z. Lum, M. Sitti, Soft actuators for small-scale robotics. *Adv. Mater.* **29**, 1603483 (2017).
8. C. Majidi, Soft robotics: A perspective—Current trends and prospects for the future. *Soft Robot.* **1**, 5–11 (2014).
9. S. Kim, C. Laschi, B. Trimmer, Soft robotics: A bioinspired evolution in robotics. *Trends Biotechnol.* **31**, 287–294 (2013).
10. C. Ohm, M. Brehmer, R. Zentel, Liquid crystalline elastomers as actuators and sensors. *Adv. Mater.* **22**, 3366–3387 (2010).
11. W. H. de Jeu, *Liquid Crystal Elastomers: Materials and Applications* (Springer, 2012), vol. 250.
12. M. Warner, E. M. Terentjev, *Liquid Crystal Elastomers* (Oxford Univ. Press, 2007).
13. T. J. White, Photomechanical effects in liquid crystalline polymer networks and elastomers. *J. Polym. Sci. B* **56**, 695–705 (2018).
14. Y. Yu, T. Ikeda, Soft actuators based on liquid-crystalline elastomers. *Angew. Chem. Int. Ed.* **45**, 5416–5418 (2006).
15. H. Jiang, C. Li, X. Huang, Actuators based on liquid crystalline elastomer materials. *Nanoscale* **5**, 5225–5240 (2013).
16. X. Lu, S. Guo, X. Tong, H. Xia, Y. Zhao, Tunable photocontrolled motions using stored strain energy in malleable azobenzene liquid crystalline polymer actuators. *Adv. Mater.* **29**, 1606467 (2017).
17. Y.-Y. Xiao, Z.-C. Jiang, X. Tong, Y. Zhao, Biomimetic locomotion of electrically powered "Janus" soft robots using a liquid crystal polymer. *Adv. Mater.* **31**, e1903452 (2019).
18. L. T. de Haan, J. M. N. Verjans, D. J. Broer, C. W. M. Bastiaansen, A. P. H. J. Schenning, Humidity-responsive liquid crystalline polymer actuators with an asymmetry in the molecular trigger that bend, fold, and curl. *J. Am. Chem. Soc.* **136**, 10585–10588 (2014).
19. M. Dai, O. T. Picot, J. M. Verjans, L. T. de Haan, A. P. Schenning, T. Peijs, C. W. Bastiaansen, Humidity-responsive bilayer actuators based on a liquid-crystalline polymer network. *ACS Appl. Mater. Interfaces* **5**, 4945–4950 (2013).
20. Z. Li, Y. Yang, Z. Wang, X. Zhang, Q. Chen, X. Qian, N. Liu, Y. Wei, Y. Ji, Polydopamine nanoparticles doped in liquid crystal elastomers for producing dynamic 3D structures. *J. Mater. Chem. A* **5**, 6740–6746 (2017).
21. M. Wang, B.-P. Lin, H. Yang, A plant tendril mimic soft actuator with phototunable bending and chiral twisting motion modes. *Nat. Commun.* **7**, 13981 (2016).
22. B. Zuo, M. Wang, B.-P. Lin, H. Yang, Photomodulated tricolor-changing artificial flowers. *Chem. Mater.* **30**, 8079–8088 (2018).
23. L. Yu, H. Shahsavan, G. Rivers, C. Zhang, P. Si, B. Zhao, Programmable 3D shape changes in liquid crystal polymer networks of uniaxial orientation. *Adv. Funct. Mater.* **28**, 1802809 (2018).
24. M. O. Saed, A. H. Torbati, C. A. Starr, R. Visvanathan, N. A. Clark, C. M. Yakacki, Thiol-acrylate main-chain liquid-crystalline elastomers with tunable thermomechanical properties and actuation strain. *J. Polym. Sci. B* **55**, 157–168 (2017).
25. M. O. Saed, A. H. Torbati, D. P. Nair, C. M. Yakacki, Synthesis of programmable main-chain liquid-crystalline elastomers using a two-stage thiol-acrylate reaction. *J. Vis. Exp.* **2016**, e53546 (2016).
26. A. Azoug, V. Vasconcellos, J. Dooling, M. Saed, C. Yakacki, T. Nguyen, Viscoelasticity of the polydomain-monodomain transition in main-chain liquid crystal elastomers. *Polymer* **98**, 165–171 (2016).
27. C. Ahn, X. Liang, S. Cai, Inhomogeneous stretch induced patterning of molecular orientation in liquid crystal elastomers. *Extreme Mech. Lett.* **5**, 30–36 (2015).
28. C. M. Yakacki, M. Saed, D. P. Nair, T. Gong, S. M. Reed, C. N. Bowman, Tailorable and programmable liquid-crystalline elastomers using a two-stage thiol–acrylate reaction. *RSC Adv.* **5**, 18997–19001 (2015).
29. X. Zheng, S. Guan, C. Zhang, T. Qu, W. Wen, Y. Zhao, A. Chen, A cut-and-weld process to 3d architectures from multiresponsive crosslinked liquid crystalline polymers. *Small* **15**, e1900110 (2019).
30. Y. Xia, X. Zhang, S. Yang, Instant locking of molecular ordering in liquid crystal elastomers by oxygen-mediated thiol–acrylate click reactions. *Angew. Chem. Int. Ed.* **57**, 5665–5668 (2018).
31. H. Yang, M.-X. Liu, Y.-W. Yao, P.-Y. Tao, B.-P. Lin, P. Keller, X.-Q. Zhang, Y. Sun, L.-X. Guo, Polysiloxane-based liquid crystalline polymers and elastomers prepared by thiol–ene chemistry. *Macromolecules* **46**, 3406–3416 (2013).
32. Z. Wang, H. Tian, Q. He, S. Cai, Reprogrammable, reprocessible, and self-healable liquid crystal elastomer with exchangeable disulfide bonds. *ACS Appl. Mater. Interfaces* **9**, 33119–33128 (2017).
33. T. Hessberger, L. Braun, R. Zentel, Microfluidic synthesis of actuating microparticles from a thiol-ene based main-chain liquid crystalline elastomer. *Polymers* **8**, 410 (2016).
34. A. H. Gelebart, M. Mc Bride, A. P. H. J. Schenning, C. N. Bowman, D. J. Broer, Photoresponsive fiber array: Toward mimicking the collective motion of cilia for transport applications. *Adv. Funct. Mater.* **26**, 5322–5327 (2016).
35. T. H. Ware, Z. P. Perry, C. M. Middleton, S. T. Iacono, T. J. White, Programmable liquid crystal elastomers prepared by thiol–ene photopolymerization. *ACS Macro Lett.* **4**, 942–946 (2015).

Acknowledgments

Funding: This work was supported by the National Natural Science Foundation of China (nos. 51722303, 21674057, and 21788102). **Author contributions:** Y.Z., Z.W., Y.J., and Y.We. developed the idea. Y.Z. and Z.W. performed the experiments. Y.Z. and Y.J. wrote the paper and designed the figures. All other authors were involved in certain aspects of the experiments. **Competing interests:** The authors declare that they have no competing interests. **Data and materials availability:** All data needed to evaluate the conclusions in the paper are present in the paper and/or the Supplementary Materials. Additional data related to this paper may be requested from the authors.

Submitted 25 July 2019
Accepted 5 December 2019
Published 28 February 2020
10.1126/sciadv.aay8606

Citation: Y. Zhang, Z. Wang, Y. Yang, Q. Chen, X. Qian, Y. Wu, H. Liang, Y. Xu, Y. Wei, Y. Ji, Seamless multimaterial 3D liquid-crystalline elastomer actuators for next-generation entirely soft robots. *Sci. Adv.* **6**, eaay8606 (2020).